

X-ray spectroscopic study on transition metal oxide-based catalysts and battery materials

Z. Hu[#] and L.H. Tjeng^{##}

Using *in-situ/in-operando* and *ex-situ* x-ray absorption spectroscopy (XAS), we have investigated transition metal oxide-based catalysts for water splitting and CO₂ reduction, as well as transition metal oxide battery materials for energy storage. These studies aim to the development of promising solutions for mitigating global warming and reducing environmental pollution.

Over the past three years, we have intensified our efforts to investigate transition metal oxide-based catalysts and battery materials using synchrotron radiation-based spectroscopies. Our primary objective is to understand the electronic states of transition metal ions during various operational processes. Leveraging our long-standing expertise in soft X-ray absorption spectroscopy (soft-XAS), we ensure not only the reliable and precise acquisition of experimental data but also the detailed and nuanced analysis of the resulting spectra. These efforts are further supported by our extensive database of energy-calibrated reference spectra, accumulated over the past 30 years

We analyzed the spectra using configuration-interaction (CI) calculations that include full atomic-multiplet theory. CI is essential for accurately capturing covalency in these strongly correlated systems, as covalency reflects the presence of ligand hole states, which play a pivotal role in catalytic processes and the charging-discharging cycles of batteries. Incorporating full atomic-multiplet theory is crucial not only for accurately representing the energy structure of the soft-XAS final states but also for deriving the correct total energy level diagram for the ground and initial state configurations.

We collaborated closely with partners specializing in catalyst and battery research, focusing on systems that align with our expertise in soft-XAS and transition metal compounds. In most cases, we successfully extracted detailed information about the charge, orbital, and spin states of the ions. Our work in this field has led to over 130 publications during the 2021–2024 census period, marking a significant increase compared to the 2018–2021 period. This growth reflects the rising interest within the scientific community in leveraging our expertise. Notably, 29 of these 130 publications appeared in journals with an impact factor greater than 20, including 14 in Nature Communications [1–43].

Protective coating of LiNiO₂ for all-solid-state-lithium-battery applications [2]

To illustrate our achievements, we highlighted in the main report our spectroscopic study of LiNiO₂ as cat-

alyst for oxygen evolution reaction (OER) [35]. Here, we present our other study on LiNiO₂, this time as a material in an all-solid-state lithium battery (ASSLB) [2]. LiNiO₂ has not yet achieved commercial success in conventional lithium-ion batteries due to its severe thermal instability when paired with flammable liquid electrolytes. This significant drawback can lead to thermal runaway, particularly in the charged (delithiated) state. In contrast, ASSLBs use solid electrolytes and eliminate the need for volatile, flammable solvents, offering superior safety features. As a result, ASSLBs may enable the adoption of high-energy LiNiO₂ cathodes for commercial applications.

Among the various types of solid electrolytes, sulfide solid electrolytes are the most suitable for use in all-solid-state batteries for electromobility, where both high energy and high power densities are required. Unfortunately, the most promising sulfide solid electrolytes have a narrow electrochemical stability window, which limits their compatibility with high-voltage cathodes. A promising approach to overcoming this challenge is coating high-voltage cathodes with chemically compatible, stable buffering layers that have high ionic conductivity but low electronic conductivity. However, the most commonly used coating layers in high-performance ASSLBs often rely on expensive elements (e.g., Nb, Ta, La, and Zr) to achieve the necessary ionic conductivity. In this study, our collaborators investigated the low-cost ultrathin Li_xAl_xZn_zO_δ (LAZO) protective layer as a coating material for the LiNiO₂ cathode. We analyzed the chemical stability of the system using soft X-ray absorption spectroscopy (soft-XAS).

The purple curve in Fig. 1a shows the Ni *L*_{2,3} XAS spectrum of pristine LiNiO₂, which is nearly identical to the Ni³⁺ spectrum (primarily 3*d*⁸*L* character) of LiNiO₂ observed in the OER experiment [35], as shown by the black curve in Fig. 1c. The purple curve in Fig. 1b displays the spectrum of LiNiO₂ protected by LAZO. Although it appears similar to the pristine case at first glance, the ratio of peak A to peak B has increased slightly. Since the NiO spectrum has its main peak only 0.29 eV below peak A (see blue curve in

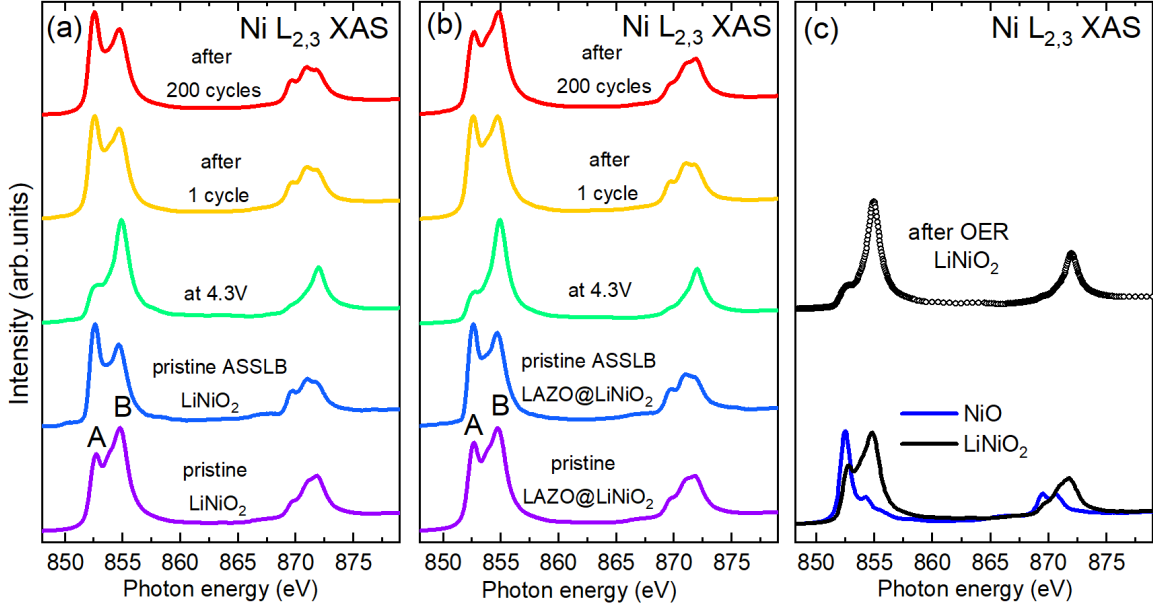


Fig. 1: Ni $L_{2,3}$ soft x-ray absorption (XAS) spectra of (a) unprotected LiNiO_2 and (b) $\text{Li}_x\text{Al}_y\text{Zn}_z\text{O}_\delta$ (LAZO)-coated LiNiO_2 under various conditions (see text). Panel (c) displays the spectra of LiNiO_2 in an OER set-up and of NiO as a Ni^{2+} reference material.

Fig. 1c), we attribute the increase in peak A to the formation of Ni^{2+} ions, suggesting that the deposition of the LAZO overlayer caused a chemical reaction with the LiNiO_2 . Upon assembling the ASSLB device, peak A further increases for both the unprotected LiNiO_2 (Fig. 1a) and the LAZO-coated LiNiO_2 (Fig. 1b), indicating further chemical reactions that additionally convert Ni^{3+} to Ni^{2+} in the cathode material.

Charging the devices to 4.3 V brings the LAZO-coated LiNiO_2 to the same chemical state as the LiNiO_2 after the OER experiment, while the uncoated LiNiO_2 shows a slight change in valence state due to side chemical/electrochemical reactions with the solid electrolytes. This can be seen by comparing the green curves in Fig. 1a and 1b with the black dotted curve in Fig. 1c. The spectrum consists of roughly 75% Ni^{4+} ($3d^8\bar{L}^2$) and 25% Ni^{3+} ($3d^8\bar{L}$) species in the cathode material [35]. Discharging the device returns the cathode material to its Ni^{3+} state, as shown by the yellow curves in Fig. 1a and 1b. However, the amount of Ni^{2+} species strongly depends on whether the cathode material is unprotected or covered by LAZO. After 200 cycles of charging and discharging, the effect of the LAZO overlayer becomes clear: the LiNiO_2 cathode material remains in the same chemical state as it was in the pristine condition, while the unprotected LiNiO_2 cathode shows a significant amount of Ni^{2+} species, indicating permanent damage to the device. This study demonstrates that LAZO is a promising low-cost protective layer that can make LiNiO_2 -based ASSLBs suitable for commercial applications.

Evolution of defect-rich Co_3O_4 cathode material under OER conditions [44]

Another example of how our long-standing expertise in soft-XAS can aid in analyzing changes in the chemical state of a catalyst material under *in-operando* conditions is our study on defect-rich Co_3O_4 (D- Co_3O_4) nanosheets for OER applications [44]. D- Co_3O_4 has been widely reported as an advanced OER electrocatalyst; however, the role of the defects has not yet been fully understood. In this study, we investigated the evolution of the material by performing an *in-operando* soft-XAS experiment, which is challenging because it requires designing and operating an instrument capable of separating the liquid from the ultrahigh vacuum.

Stoichiometric Co_3O_4 bulk spinel has an average Co valence of 2.67+, with two Co^{3+} ions octahedrally coordinated by oxygen ions and one Co^{2+} ion tetrahedrally coordinated. In contrast, D- Co_3O_4 nanosheets under *in-operando* conditions exhibit a significantly different charge state. This is already evident at open-circuit potential (OCP). Figure 2a shows the Co $L_{2,3}$ XAS spectrum of the material, alongside the (weighted) spectra of CoO , $\text{YBaCo}_3\text{AlO}_7$ [45], and $\text{Li}_2\text{Co}_2\text{O}_4$ [46]. Here, CoO represents an octahedrally coordinated high-spin Co^{2+} system, $\text{YBaCo}_3\text{AlO}_7$ represents a tetrahedral high-spin Co^{2+} system, and $\text{Li}_2\text{Co}_2\text{O}_4$ represents an octahedral low-spin Co^{3+} system. Under open-circuit potential, the spectrum of D- Co_3O_4 can be reproduced with about 15%, 35%, and 48% respective contributions, yielding an average Co valence of 2.44+.

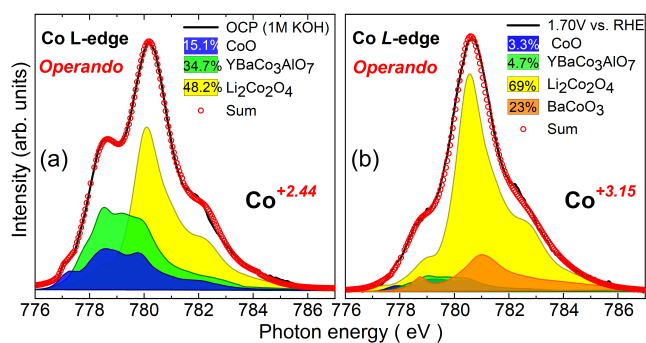


Fig. 2: Co $L_{2,3}$ soft x-ray absorption (XAS) spectra of defect-rich Co_3O_4 nanosheets in-operando: (left panel) under open-circuit-potential (OCP) and (right panel) at 1.70 V potential. Spectra of CoO, $\text{YBaCo}_3\text{AlO}_7$, $\text{Li}_2\text{Co}_2\text{O}_4$, and BaCoO_3 are included as reference.

Under OER conditions, i.e., at a 1.70 V potential vs. RHE, the D- Co_3O_4 nanosheet spectrum undergoes significant changes, as shown in Fig. 2b. To analyze the data, we include the spectrum of BaCoO_3 as a reference for an octahedrally coordinated low-spin Co^{4+} system [47]. The weights of the reference spectra in the simulation that reproduces the spectrum are approximately 3%, 5%, 69%, and 23%, respectively. The average Co valence in the D- Co_3O_4 nanosheet material under OER conditions is about 3.15+. Furthermore, the simulation indicates that the tetrahedrally coordinated Co ions have almost disappeared, and that thus the material has undergone an irreversible change during the OER process.

External Cooperation Partners

Chang-Yang Kuo (National Yang Ming Chiao Tung University, Taiwan); Chien-Te Chen (National Synchrotron Radiation Research Center, 101 Hsin-Ann Road, Hsinchu 30077, Taiwan); Peter G. Bruce (University of Oxford, United Kingdom); Doron Aurbach (Bar-Ilan University, Israel); Jian-Qiang Wang and Linjuan Zhang (Shanghai Institute of Applied Physics, Chinese Academy of Sciences, China).

References

- [1]* *Stabilization of layered lithium-rich manganese oxide for anion exchange membrane fuel cells and water electrolyzers*, X. Zhong, L. Sui, M. Yang, T. Koketsu, M. Klingenhof, S. Selve, K. G. Reeves, C. Ge, L. Zhuang, W. H. Kan, M. Avdeev, M. Shu, N. Alonso-Vante, J.-M. Chen, S.-C. Haw, C.-W. Pao, Y.-C. Chang, Y. Huang, Z. Hu, P. Strasser, and J. Ma, *Nature Catalysis* 7 (2024) 546, <https://dx.doi.org/10.1038/s41929-024-01136-1>
- [2]* *High-energy all-solid-state lithium batteries enabled by Co-free LiNiO_2 cathodes with robust outside-in structures.*, L. Wang, A. Mukherjee, C. Y. Kuo, R. Chakrabarty, S. an Yemini, A. A. Dameron, J. W. DuMont, S. H. Akella, A. Saha, S. Taragin, H. Aviv, D. Naveh, D. Sharon, T. S. Chan, H. J. Lin, J. F. Lee, C. T. Chen, B. Liu, X. Gao, S. Basu, Z. Hu, D. Aurbach, P. G. Bruce, and M. Noked, *Nature Nanotechnol.* 19 (2024) 208, <https://dx.doi.org/10.1038/s41565-023-01519-8>
- [3]* *Regioselective epitaxial growth of metallic heterostructures.*, X. Huang, J. Feng, S. Hu, B. Xu, M. Hao, X. Liu, Y. Wen, D. Su, Y. Ji, Y. Li, Y. Li, Y. Huang, T.-S. Chan, Z. Hu, N. Tian, Q. Shao, and X. Huang, *Nature Nanotechnol.* 19 (2024) 1306, <https://dx.doi.org/10.1038/s41565-024-01696-0>
- [4]* *Extraordinary acidic oxygen evolution on new phase 3R-iridium oxide*, Z. Fan, Y. Ji, Q. Shao, S. Geng, W. Zhu, Y. Liu, F. Liao, Z. Hu, Y.-C. Chang, C.-W. Pao, Y. Li, Z. Kang, and M. Shao, *Joule* 5 (2021) 3221, <https://dx.doi.org/https://doi.org/10.1016/j.joule.2021.10.002>
- [5]* *Oxygen vacancy chemistry in oxide cathodes*, Y.-H. Zhang, S. Zhang, N. Hu, Y. Liu, J. Ma, P. Han, Z. Hu, X. Wang, and G. Cui, *Chem. Soc. Rev.* 53 (2024) 3302, <https://dx.doi.org/10.1039/D3CS00872J>
- [6]* *Three-dimensional porous platinum-tellurium-rhodium surface/interface achieve remarkable practical fuel cell catalysis*, L. Bu, F. Ning, J. Zhou, C. Zhan, M. Sun, L. Li, Y. Zhu, Z. Hu, Q. Shao, X. Zhou, B. Huang, and X. Huang, *Energy Environ. Sci.* 15 (2022) 3877, <https://dx.doi.org/10.1039/D2EE01597H>
- [7]* *Surface and lattice engineered ruthenium superstructures towards high-performance bifunctional hydrogen catalysis*, L. Li, S. Liu, C. Zhan, Y. Wen, Z. Sun, J. Han, T.-S. Chan, Q. Zhang, Z. Hu, and X. Huang, *Energy Environ. Sci.* 16 (2023) 157, <https://dx.doi.org/10.1039/D2EE02076A>
- [8]* *In situ-polymerized lithium salt as a polymer electrolyte for high-safety lithium metal batteries*, S. Zhang, F. Sun, X. Du, X. Zhang, L. Huang, J. Ma, S. Dong, A. Hilger, I. Manke, L. Li, B. Xie, J. Li, Z. Hu, A. C. Komarek, H.-J. Lin, C.-Y. Kuo, C.-T. Chen, P. Han, G. Xu, Z. Cui, and G. Cui, *Energy Environ. Sci.* 16 (2023) 2591, <https://dx.doi.org/10.1039/D3EE00558E>
- [9]* *Exceptionally Robust Face-Sharing Motifs Enable Efficient and Durable Water Oxidation*, D. Guan, K. Zhang, Z. Hu, X. Wu, J.-L. Chen, C.-W. Pao, Y. Guo, W. Zhou, and Z. Shao, *Adv. Mater.* 33 (2021) 2103392, <https://dx.doi.org/https://doi.org/10.1002/adma.202103392>
- [10]* *Compensating Electronic Effect Enables Fast Site-to-Site Electron Transfer over Ultrathin RuMn Nanosheet Branches toward Highly Electroactive and Stable Water Splitting*, L. Li, L. Bu, B. Huang, P. Wang, C. Shen, S. Bai, T.-S. Chan, Q. Shao, Z. Hu, and X. Huang, *Adv.*

- Mater.* **33** (2021) 2105308, <https://dx.doi.org/https://doi.org/10.1002/adma.202105308>
- [11]* *Enabling Anionic Redox Stability of P2-Na₅/6Li₁/4Mn₃/4O₂ by Mg Substitution*, Y. Huang, Y. Zhu, A. Nie, H. Fu, Z. Hu, X. Sun, S.-C. Haw, J.-M. Chen, T.-S. Chan, S. Yu, G. Sun, G. Jiang, J. Han, W. Luo, and Y. Huang, *Advanced Materials* **34** (2022) 2105404, <https://dx.doi.org/https://doi.org/10.1002/adma.202105404>
- [12]* *Spin-Polarization Strategy for Enhanced Acidic Oxygen Evolution Activity*, L. Li, J. Zhou, X. Wang, J. Gracia, M. Valvidares, J. Ke, M. Fang, C. Shen, J.-M. Chen, Y.-C. Chang, C.-W. Pao, S.-Y. Hsu, J.-F. Lee, A. Ruotolo, Y. Chin, Z. Hu, X. Huang, and Q. Shao, *Adv. Mater.* **35** (2023) 2302966, <https://dx.doi.org/https://doi.org/10.1002/adma.202302966>
- [13]* *Identifying a Universal Activity Descriptor and a Unifying Mechanism Concept on Perovskite Oxides for Green Hydrogen Production*, D. Guan, H. Xu, Q. Zhang, Y.-C. Huang, C. Shi, Y.-C. Chang, X. Xu, J. Tang, Y. Gu, C.-W. Pao, S.-C. Haw, J.-M. Chen, Z. Hu, M. Ni, and Z. Shao, *Adv. Mater.* **35** (2023) 2305074, <https://dx.doi.org/https://doi.org/10.1002/adma.202305074>
- [14]* *Structurally-Distorted RuIr-Based Nanoframes for Long-Duration Oxygen Evolution Catalysis*, S. Liu, H. Tan, Y.-C. Huang, Q. Zhang, H. Lin, L. Li, Z. Hu, W.-H. Huang, C.-W. Pao, J.-F. Lee, Q. Kong, Q. Shao, Y. Xu, and X. Huang, *Adv. Mater.* **35** (2023) 2305659, <https://dx.doi.org/https://doi.org/10.1002/adma.202305659>
- [15]* *3D Noble-Metal Nanostructures Approaching Atomic Efficiency and Atomic Density Limits*, S. Liu, W.-H. Huang, S. Meng, K. Jiang, J. Han, Q. Zhang, Z. Hu, C.-W. Pao, H. Geng, X. Huang, C. Zhan, Q. Yun, Y. Xu, and X. Huang, *Adv. Mater.* **36** (2024) 2312140, <https://dx.doi.org/https://doi.org/10.1002/adma.202312140>
- [16]* *Core-Shell Design of Metastable Phase Catalyst Enables Highly-Performance Selective Hydrogenation*, J. Su, Y. Ji, S. Geng, L. Li, D. Liu, H. Yu, B. Song, Y. Li, C.-W. Pao, Z. Hu, X. Huang, J. Lu, and Q. Shao, *Adv. Mater.* **36** (2024) 2308839, <https://dx.doi.org/https://doi.org/10.1002/adma.202308839>
- [17]* *Augmented Electrochemical Oxygen Evolution by d-p Orbital Electron Coupling*, N. Sun, Z. Zheng, Z. Lai, J. Wang, P. Du, T. Ying, H. Wang, J. Xu, R. Yu, Z. Hu, C.-W. Pao, W.-H. Huang, K. Bi, M. Lei, and K. Huang, *Adv. Mater.* **36** (2024) 2404772, <https://dx.doi.org/https://doi.org/10.1002/adma.202404772>
- [18]* *Bidirectionally Compatible Buffering Layer Enables Highly Stable and Conductive Interface for 4.5V Sulfide-Based All-Solid-State Lithium Batteries*, L. Wang, X. Sun, J. Ma, B. Chen, C. Li, J. Li, L. Chang, X. Yu, T.-S. Chan, Z. Hu, M. Noked, and G. Cui, *Adv. Energy Mater.* **11** (2021) 2100881, <https://dx.doi.org/https://doi.org/10.1002/aenm.202100881>
- [19]* *Stabilization of Lattice Oxygen in Li-Rich Mn-Based Oxides via Swing-like Non-Isothermal Sintering*, Y.-H. Zhang, D. Zhang, L.-R. Wu, J. Ma, Q. Yi, Z. Wang, X. Wang, Z. Wu, C. Zhang, N. Hu, S.-C. Haw, J.-M. Chen, Z. Hu, and G. Cui, *Advanced Energy Materials* **12** (2022) 2202341, <https://dx.doi.org/https://doi.org/10.1002/aenm.202202341>
- [20]* *Revealing the importance of suppressing formation of lithium hydride and hydrogen in Li anode protection*, G. Xu, X. Du, S. Zhang, J. Li, S. Dong, Z. Hu, and G. Cui, *Interdisciplinary Materials* **2** (2023) 337, <https://dx.doi.org/https://doi.org/10.1002/idm2.12078>
- [21]* *Unraveling the Spatial Asynchronous Activation Mechanism of Oxygen Redox-Involved Cathode for High-Voltage Solid-State Batteries*, N. Hu, Y.-H. Zhang, Y. Yang, H. Wu, Y. Liu, C. Hao, Y. Zheng, D. Sun, W. Li, J. Li, Z. Hu, T.-S. Chan, C.-W. Kao, Q. Kong, X. Wang, S.-C. Haw, J. Ma, and G. Cui, *Adv. Energy Mater.* **14** (2024) 2303797, <https://dx.doi.org/https://doi.org/10.1002/aenm.202303797>
- [22]* *High-Entropy Phase Stabilization Engineering Enables High-Performance Layered Cathode for Sodium-Ion Batteries*, B. Wang, J. Ma, K. Wang, D. Wang, G. Xu, X. Wang, Z. Hu, C.-W. Pao, J.-L. Chen, L. Du, X. Du, and G. Cui, *Adv. Energy Mater.* **14** (2024) 2401090, <https://dx.doi.org/https://doi.org/10.1002/aenm.202401090>
- [23]* *Boosting ethanol oxidation by NiOOH-CuO nano-heterostructure for energy-saving hydrogen production and biomass upgrading*, H. Sun, L. Li, Y. Chen, H. Kim, X. Xu, D. Guan, Z. Hu, L. Zhang, Z. Shao, and W. Jung, *Appl. Catal., B* **325** (2023) 122388, <https://dx.doi.org/https://doi.org/10.1016/j.apcatb.2023.122388>
- [24]* *Synergistic effects in ordered Co oxides for boosting catalytic activity in advanced oxidation processes*, M. Zhu, D. Guan, Z. Hu, H.-J. Lin, C.-T. Chen, H.-S. Sheu, S. Wang, J. Zhou, W. Zhou, and Z. Shao, *Appl. Catal., B* **297** (2021) 120463, <https://dx.doi.org/https://doi.org/10.1016/j.apcatb.2021.120463>
- [25]* *Exceptional lattice-oxygen participation on artificially controllable electrochemistry-induced crystalline-amorphous phase to boost oxygen-evolving performance*, H. Zhang, D. Guan, Z. Hu, Y.-C. Huang, X. Wu, J. Dai, C.-L. Dong, X. Xu, H.-J. Lin, C.-T. Chen, W. Zhou, and Z. Shao, *Applied Catalysis B: Environmental* **297** (2021) 120484, <https://dx.doi.org/https://doi.org/10.1016/j.apcatb.2021.120484>
- [26]* *Large current density for oxygen evolution from pyramidally-coordinated Co oxide*, Y. Hu, L. Li, J. Zhao, Y.-C. Huang, C. Yang Kuo, J. Zhou, Y. Fan, H.-J. Lin, C.-L. Dong, C.-W. Pao, J.-F. Lee, C.-T. Chen, C. Jin, Z. Hu, J.-Q. Wang, and L. Zhang, *Appl Catal B-Environ Energy* **333** (2023) 122785, <https://dx.doi.org/https://doi.org/10.1016/j.apcatb.2023.122785>
- [27]* *Palladium chalcogenide nanosheets with p-d orbital hybridization for enhanced alcohol electro-oxidation performance*, L. Wang, Z. Yu, W. Yan, L. Liu, M. Wang, Q. Kong, Z. Hu, H. Geng, X. Huang, and Y. Li, *Appl.*

- Catal.*, **B 343** (2024) 123564, <https://dx.doi.org/https://doi.org/10.1016/j.apcatb.2023.123564>
- [28]* Realizing B-site high-entropy air electrode for superior reversible solid oxide cells, Z. Xia, Y. Zhang, X. Xiong, J. Cui, Z. Liu, S. Xi, Z. Hu, J.-Q. Wang, and L. Zhang, *Appl Catal B-Environ Energy* **357** (2024) 124314, <https://dx.doi.org/https://doi.org/10.1016/j.apcatb.2024.124314>
- [29]* Synergistic effect to unlock the activity and stability for oxygen evolution reaction in spinel LiMn_2O_4 via d-block metal substitution, J. Li, L. Liu, J. Wu, Z. Hu, Y.-Y. Chin, H.-J. Lin, C.-T. Chen, X. Pan, Y. Deng, N. Alonso-Vante, L. Sui, Y. Xie, and J. Ma, *Appl Catal B-Environ Energy* **357** (2024) 124331, <https://dx.doi.org/https://doi.org/10.1016/j.apcatb.2024.124331>
- [30]* Boosting oxygen reduction activity and enhancing stability through structural transformation of layered lithium manganese oxide, X. Zhong, M. Oubla, X. Wang, Y. Huang, H. Zeng, S. Wang, K. Liu, J. Zhou, L. He, H. Zhong, N. Alonso-Vante, C.-W. Wang, W.-B. Wu, H.-J. Lin, C.-T. Chen, Z. Hu, Y. Huang, and J. Ma, *Nat. Commun.* **12** (2021) 3136, <https://dx.doi.org/10.1038/s41467-021-23430-3>
- [31]* A top-down strategy for amorphization of hydroxyl compounds for electrocatalytic oxygen evolution, S. Liu, S. Geng, L. Li, Y. Zhang, G. Ren, B. Huang, Z. Hu, J.-F. Lee, Y.-H. Lai, Y.-H. Chu, Y. Xu, Q. Shao, and X. Huang, *Nat. Commun.* **13** (2022) 1187, <https://dx.doi.org/10.1038/s41467-022-28888-3>
- [32]* Hydrogen spillover in complex oxide multifunctional sites improves acidic hydrogen evolution electrocatalysis, J. Dai, Y. Zhu, Y. Chen, X. Wen, M. Long, X. Wu, Z. Hu, D. Guan, X. Wang, C. Zhou, Q. Lin, Y. Sun, S.-C. Weng, H. Wang, W. Zhou, and Z. Shao, *Nat. Commun.* **13** (2022), <https://dx.doi.org/10.1038/s41467-022-28843-2>
- [33]* Coupling of nanocrystal hexagonal array and two-dimensional metastable substrate boosts H_2 -production, Z. Fan, F. Liao, Y. Ji, Y. Liu, H. Huang, D. Wang, K. Yin, H. Yang, M. Ma, W. Zhu, M. Wang, Z. Kang, Y. Li, M. Shao, Z. Hu, and Q. Shao, *Nat. Commun.* **13** (2022), <https://dx.doi.org/10.1038/s41467-022-33512-5>
- [34]* Iridium single atoms incorporated in Co_3O_4 efficiently catalyze the oxygen evolution in acidic conditions, Y. Zhu, J. Wang, T. Koketsu, M. Kroschel, J.-M. Chen, S.-Y. Hsu, G. Henkelman, Z. Hu, P. Strasser, and J. Ma, *Nat. Commun.* **13** (2022), <https://dx.doi.org/10.1038/s41467-022-35426-8>
- [35]* Unusual double ligand holes as catalytic active sites in LiNiO_2 , H. Huang, Y.-C. Chang, Y.-C. Huang, L. Li, A. C. Komarek, L. H. Tjeng, Y. Orikasa, C.-W. Pao, T.-S. Chan, J.-M. Chen, S.-C. Haw, J. Zhou, Y. Wang, H.-J. Lin, C.-T. Chen, C.-L. Dong, C.-Y. Kuo, J.-Q. Wang, Z. Hu, and L. Zhang, *Nat. Commun.* **14** (2023) 2112, <https://dx.doi.org/10.1038/s41467-023-37775-4>
- [36]* Zhang-Rice singlets state formed by two-step oxidation for triggering water oxidation under operando conditions, C.-K. Peng, Y.-C. Lin, C.-L. Chiang, Z. Qian, Y.-C. Huang, C.-L. Dong, J.-F. Li, C.-T. Chen, Z. Hu, S.-Y. Chen, and Y.-G. Lin, *Nat. Commun.* **14** (2023) 529, <https://dx.doi.org/10.1038/s41467-023-36317-2>
- [37]* Self-organized hetero-nanodomains actuating super Li^+ conduction in glass ceramics, Y. Wang, H. Qu, B. Liu, X. Li, J. Ju, J. Li, S. Zhang, J. Ma, C. Li, Z. Hu, C.-K. Chang, H.-S. Sheu, L. Cui, F. Jiang, E. R. H. van Eck, A. P. M. Kentgens, G. Cui, and L. Chen, *Nat. Commun.* **14** (2023), <https://dx.doi.org/10.1038/s41467-023-35982-7>
- [38]* Atomic-thick metastable phase RhMo nanosheets for hydrogen oxidation catalysis, J. Zhang, X. Liu, Y. Ji, X. Liu, D. Su, Z. Zhuang, Y.-C. Chang, C.-W. Pao, Q. Shao, Z. Hu, and X. Huang, *Nat. Commun.* **14** (2023), <https://dx.doi.org/10.1038/s41467-023-37406-y>
- [39]* Sintering-induced cation displacement in protonic ceramics and way for its suppression, Z. Liu, Y. Song, X. Xiong, Y. Zhang, J. Cui, J. Zhu, L. Li, J. Zhou, C. Zhou, Z. Hu, G. Kim, F. Ciucci, Z. Shao, J.-Q. Wang, and L. Zhang, *Nat. Commun.* **14** (2023), <https://dx.doi.org/10.1038/s41467-023-43725-x>
- [40]* Spin polarized $\text{Fe}_1\text{-Ti}$ pairs for highly efficient electroreduction nitrate to ammonia, J. Dai, Y. Tong, L. Zhao, Z. Hu, C.-T. Chen, C.-Y. Kuo, G. Zhan, J. Wang, X. Zou, Q. Zheng, W. Hou, R. Wang, K. Wang, R. Zhao, X.-K. Gu, Y. Yao, and L. Zhang, *Nat. Commun.* **15** (2024), <https://dx.doi.org/10.1038/s41467-023-44469-4>
- [41]* Synergistic dual-phase air electrode enables high and durable performance of reversible proton ceramic electrochemical cells, Z. Liu, Y. Bai, H. Sun, D. Guan, W. Li, W.-H. Huang, C.-W. Pao, Z. Hu, G. Yang, Y. Zhu, R. Ran, W. Zhou, and Z. Shao, *Nat. Commun.* **15** (2024), <https://dx.doi.org/10.1038/s41467-024-44767-5>
- [42]* Implanting oxophilic metal in PtRu nanowires for hydrogen oxidation catalysis, Z. Huang, S. Hu, M. Sun, Y. Xu, S. Liu, R. Ren, L. Zhuang, T.-S. Chan, Z. Hu, T. Ding, J. Zhou, L. Liu, M. Wang, Y.-C. Huang, N. Tian, L. Bu, B. Huang, and X. Huang, *Nat. Commun.* **15** (2024), <https://dx.doi.org/10.1038/s41467-024-45369-x>
- [43]* Facilitating alkaline hydrogen evolution reaction on the hetero-interfaced Ru/RuO_2 through Pt single atoms doping, Y. Zhu, M. Klingenhof, C. Gao, T. Koketsu, G. Weiser, Y. Pi, S. Liu, L. Sui, J. Hou, J. Li, H. Jiang, L. Xu, W.-H. Huang, C.-W. Pao, M. Yang, Z. Hu, P. Strasser, and J. Ma, *Nat. Commun.* **15** (2024), <https://dx.doi.org/10.1038/s41467-024-45654-9>
- [44]* In Situ/Operando Soft X-ray Spectroscopic Identification of a Co^{4+} Intermediate in the Oxygen Evolution Reaction of Defective Co_3O_4 Nanosheets, Y.-C. Huang, W. Chen, Z. Xiao, Z. Hu, Y.-R. Lu, J.-L. Chen, C.-L. Chen, H.-J. Lin, C.-T. Chen, K. T. Arul, S. Wang, C.-L. Dong, and W.-C. Chou, *J. Phys. Chem. Lett.* **13** (2022) 8386, <https://dx.doi.org/10.1021/acs.jpcclett.2c01557>

- [45] *Electronic and magnetic properties of the kagome systems $YBaCo_4O_7$ and $YBaCo_3MO_7$ ($M=Al, Fe, N$).* Hollmann, Z. Hu, M. Valldor, A. Maignan, A. Tanaka, H. H. Hsieh, H.-J. Lin, C. T. Chen, and L. H. Tjeng, *Phys. Rev. B* **80** (2009) 085111, <https://dx.doi.org/10.1103/PhysRevB.80.085111>
- [46] *Voltage- and time-dependent valence state transition in cobalt oxide catalysts during the oxygen evolution reaction,* J. Zhou, L. Zhang, Y.-C. Huang, C.-L. Dong, H.-J. Lin, C.-T. Chen, L. H. Tjeng, and Z. Hu, *Nat. Commun.* **11** (2020), <https://dx.doi.org/10.1038/s41467-020-15925-2>
- [47] *Spin-orbit coupling and crystal-field distortions for a low-spin $3d^5$ state in $BaCoO_3$,* Y. Y. Chin, Z. Hu, H.-J. Lin, S. Agrestini, J. Weinen, C. Martin, S. Hébert, A. Maignan, A. Tanaka, J. C. Cezar, N. B. Brookes, Y.-F. Liao, K.-D. Tsuei, C. T. Chen, D. I. Khomskii, and L. H. Tjeng, *Phys. Rev. B* **100** (2019) 205139, <https://dx.doi.org/10.1103/PhysRevB.100.205139>

#zhiwei.hu@cpfs.mpg.de

##hao.tjeng@cpfs.mpg.de